© 2017. Published by The Company of Biologists Ltd | Development (2017) 144, 4037-4045 doi:10.1242/dev.155176

RESEARCH ARTICLE

The Dlx5-FGF10 signaling cascade controls cranial neural crest and myoblast interaction during oropharyngeal patterning and development

Hideki Sugii[1,2], Alexandre Grimaldi[1], Jingyuan Li[1], Carolina Parada[1], Thach Vu-Ho[1], Jifan Feng[1], Junjun Jing[1,3], Yuan Yuan[1], Yuxing Guo[1,4], Hidefumi Maeda[2,5] and Yang Chai[1,*]

ABSTRACT

Craniofacial development depends on cell-cell interactions, coordinated cellular movement and differentiation under the control of regulatory gene networks, which include the distal-less (Dlx) gene family. However, the functional significance of *Dlx5* in patterning the oropharyngeal region has remained unknown. Here, we show that loss of *Dlx5* leads to a shortened soft palate and an absence of the levator veli palatini, palatopharyngeus and palatoglossus muscles that are derived from the 4th pharyngeal arch (PA); however, the tensor veli palatini, derived from the 1st PA, is unaffected. Dlx5-positive cranial neural crest (CNC) cells are in direct contact with myoblasts derived from the pharyngeal mesoderm, and *Dlx5* disruption leads to altered proliferation and apoptosis of CNC and muscle progenitor cells. Moreover, the FGF10 pathway is downregulated in *Dlx5*$^{-/-}$ mice, and activation of FGF10 signaling rescues CNC cell proliferation and myogenic differentiation in these mutant mice. Collectively, our results indicate that *Dlx5* plays crucial roles in the patterning of the oropharyngeal region and development of muscles derived from the 4th PA mesoderm in the soft palate, likely via interactions between CNC-derived and myogenic progenitor cells.

KEY WORDS: Dlx5, Soft palate, CNC cells, Myoblast, Oropharyngeal patterning, 4th pharyngeal arch

INTRODUCTION

The oropharyngeal region serves as a passage for air, water and food, and also helps to produce articulate speech, which is unique to humans. Consequently, defects in the soft palate adversely affect speech, swallowing, breathing and hearing (Precious and Delaire, 1993). The soft palate forms the posterior one-third of the palate and consists of five muscles in humans: the tensor veli palatini (TVP), levator veli palatini (LVP), palatopharyngeus (PLP), palatoglossus (PLG) and muscle of the uvula (Evans et al., 2010). Cleft of the soft palate leads to misorientation of these muscle fibers and compromises palatal function in the oropharyngeal region. Despite various surgical approaches to reorient the muscles of the soft palate in order to restore its proper function, the outcome is typically less than ideal, owing to insufficient muscle tissue and poor ability to regenerate following the operation (Carvajal Monroy et al., 2012). The lack of a more optimal approach to palatal muscle restoration is partly due to a lack of understanding of the molecular regulatory and cellular mechanisms of soft palate development.

Our recent study has shown that the anatomical structures of the soft palate and cellular contributions to them in mice are similar to those in humans, which renders the mouse an excellent model with which to study soft palate development (Grimaldi et al., 2015). Specifically, cranial neural crest (CNC)-derived cells migrate into the primordium of the soft palate and form a scaffold to guide the migration of myogenic progenitors into the soft palate, where they form the TVP, LVP, PLP and PLG (Grimaldi et al., 2015). The progenitors of these muscles in the soft palate and those in the pharynx/larynx derive from the pharyngeal mesoderm (Michailovici et al., 2015). In comparison with trunk muscle development, the molecular regulatory mechanisms underlying head muscle development are less well characterized. It is clear, however, that head muscle development is governed by both intrinsic and extrinsic programs. For example, Tbx1, Myf5, and Lhx2 form an important intrinsic genetic network to control the fate of myogenic progenitors during head muscle development (Michailovici et al., 2015). As one of the extrinsic regulators, CNC-derived cells control tongue muscle development through CNC-myogenic progenitor interactions (Han et al., 2012; Hosokawa et al., 2010).

Dlx genes play important roles in regulating craniofacial patterning and development. In mammals, six Dlx genes are expressed as convergently transcribed gene pairs, including *Dlx1*/*Dlx2*, *Dlx5*/*Dlx6* and *Dlx3*/*Dlx7*. These gene pairs have overlapping regulatory systems and expression patterns (Robledo and Lufkin, 2006). Dlx5/Dlx6 is required for establishing mandibular identity, because loss of these proteins leads to the transformation of the mandible into a maxilla (Depew et al., 2002). Hand2 restricts Dlx5/Dlx6 to the proximal domain of the mandibular arch (Barron et al., 2011). Moreover, Dlx5 controls oronasal patterning in the anterior part of the palatal shelf and indirectly regulates Shh signaling in the palatal epithelium during palatogenesis (Han et al., 2009). However, it has remained unknown where Dlx5 is expressed in the posterior part of the palate and whether Dlx5 plays a role in regulating the development of the soft palate and oropharyngeal region.

In this study, we have analyzed the expression and function of Dlx5 during the development of the posterior palate and pharyngeal region. Dlx5 is expressed in CNC cells adjacent to myogenic progenitors that are derived from the 4th pharyngeal arch. Among the soft palate muscles in *Dlx5*$^{-/-}$ mice, the TVP appeared indistinguishable from that of control mice, but the LVP, PLP and PLG were absent. Specifically, using cell-lineage tracing analysis,

[1]Center for Craniofacial Molecular Biology, University of Southern California, Los Angeles, CA 90033, USA. [2]Division of Endodontology, Kyushu University Hospital, Kyushu University, Fukuoka 812-8582, Japan. [3]State Key Laboratory of Oral Diseases, West China Hospital of Stomatology, Sichuan University, Chengdu 610041, China. [4]Department of Oral and Maxillofacial Surgery, Peking University School and Hospital of Stomatological, Beijing 100081, China. [5]Department of Endodontology and Operative Dentistry, Division of Oral Rehabilitation, Faculty of Dental Science, Kyushu University, Fukuoka 812-8582, Japan.

*Author for correspondence (ychai@usc.edu)

Y.C., 0000-0002-8943-0861

Received 19 May 2017; Accepted 21 September 2017

Development (2017) 144, 4037-4045 doi:10.1242/dev.155176

we found that Dlx5-positive CNC cells from the 4th pharyngeal arch migrated into the soft palate primordium to set up a scaffold and were adjacent to muscle progenitor cells in the LVP, PLG and PLP regions. Loss of Dlx5 also affected the proliferation and cell survival of CNC and myogenic cells in the LVP, PLG and PLP. Moreover, loss of Dlx5 resulted in decreased expression of *Fgf10*. In addition, activation of FGF10 signaling rescued differentiation of muscle progenitor cells and proliferation of CNC cells in *Dlx5*$^{-/-}$ mice. Overall, loss of Dlx5-mediated FGF10 signaling led to defects in the development of the LVP, PLG and PLP as well as patterning of the oropharyngeal region.

RESULTS

Loss of Dlx5 results in defects in the oropharyngeal region, including the soft palate

To investigate the function of Dlx5 during the development of the posterior palate, we analyzed the phenotypes of *Dlx5*$^{-/-}$ mice in the craniofacial region. Consistent with previous reports, *Dlx5*$^{-/-}$ mice exhibited a shortened soft palate with a uvula-like structure at the end (Fig. 1A,B) (Han et al., 2009). Using microCT analysis, we found that the soft palate failed to connect to the pharyngeal wall and that rugae were prominent in palates of *Dlx5*$^{-/-}$ mice (Fig. 1C,D). Next, we focused on the muscles in the soft palate region using histological analysis. In *Dlx5*$^{-/-}$ mice, the TVP was indistinguishable from that of control mice (Fig. 1E,F). In contrast, the LVP and PLG were undetectable in *Dlx5*$^{-/-}$ mice (Fig. 1G,H, data not shown). Moreover, we found that the midline region of the PLP and superior pharyngeal constrictor (SPC) were missing in *Dlx5*$^{-/-}$ mice (Fig. 1I,J; Fig. S1). These results indicate that Dlx5 is crucial for the development of soft palate and pharyngeal muscles.

To analyze where Dlx5 is expressed during development of the soft palate, we used *Dlx5-CreER;tdTomato* and *Wnt1-Cre;ZsGreen* mice to compare the distribution of Dlx5-positive cells and CNC-derived cells, respectively. In whole-mount samples, CNC-derived cells were detectable mainly in the pharyngeal arches (PAs) at early stages (E10.5, E11.5) (Fig. 2A,B) and then throughout most of the craniofacial region at later stages (E13.5, E14.5, E17.5) (Fig. 2C-E). Dlx5-positive cells were also detectable in similar, but more restricted, regions in the PAs (Fig. 2F,G), and in the craniofacial region at later stages (Fig. 2H-J). Next, we analyzed endogenous *Dlx5* expression in E16.5 *Wnt1-Cre;ZsGreen* mice and performed double staining of *ZsGreen* and *Dlx5* using RNAscope *in situ* hybridization analysis. Expression of *ZsGreen*, indicating the CNC cells, was detectable throughout the soft palate region (Fig. 2K-P). In the TVP, expression of *Dlx5* was not detectable and was only detectable in the pterygoid plate (Fig. 2K). In contrast, *Dlx5* was expressed adjacent to the muscles of the LVP and PLP (Fig. 2L,M,O,P). Moreover, *Dlx5* expression colocalized with *ZsGreen* expression in the LVP and PLP regions, but not in the TVP region (Fig. 2N-P). These results suggest that Dlx5 is expressed by a subset of CNC-derived cells during key stages of soft palate development.

Dlx5-positive CNC cells closely associate with a subgroup of myogenic progenitors in the soft palate

In order to assess whether Dlx5-positive CNC cells affect muscle development in the soft palate region, we compared Dlx5-positive cells with expression of myoblast determination protein 1 (MyoD) and myosin heavy chain (MHC). MyoD is expressed early during muscle development and acts as a muscle determination gene (Rudnicki et al., 1993). MHC is a marker of mature stages of myogenic differentiation (Chanoine et al., 1990; Parada et al., 2012). Using both of these markers allowed us to assess the possible

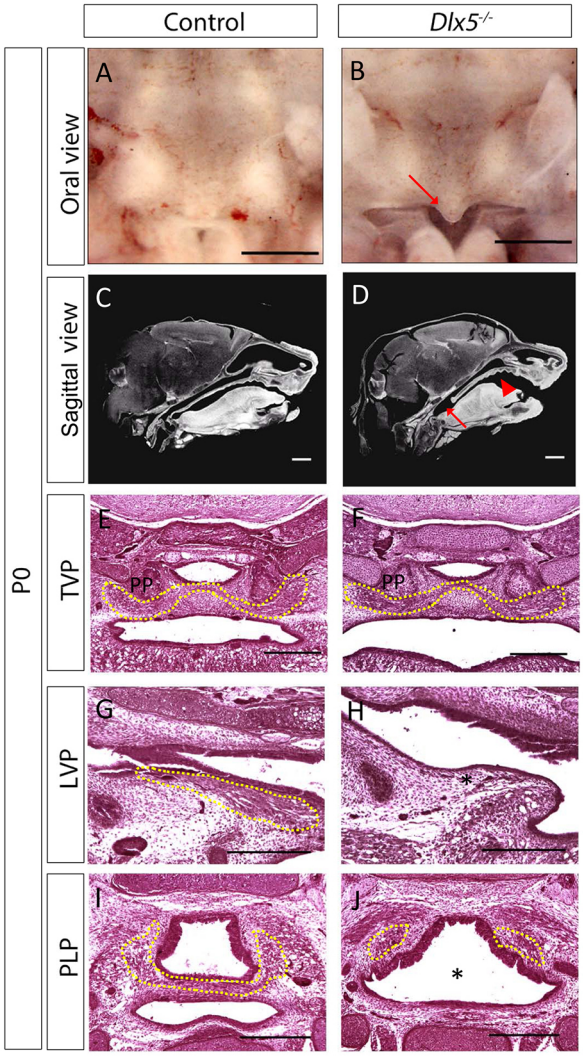

Fig. 1. Loss of Dlx5 leads to defects of craniofacial structures in the soft palate and oropharyngeal region. (A,B) Intraoral views of palates from newborn (P0) control and *Dlx5*$^{-/-}$ mice. Arrow indicates uvula-like structure. (C,D) Sagittal views of microCT scans of newborn control and *Dlx5*$^{-/-}$ mice. Arrow indicates the failure of the soft palate to connect to the pharyngeal wall and arrowhead indicates prominent rugae in *Dlx5*$^{-/-}$ mice. (E-J) Hematoxylin and Eosin staining of sections of the soft palate at the level of the TVP (E,F), LVP (G,H) and PLP (I,J) in newborn control and *Dlx5*$^{-/-}$ mice. Yellow dotted lines indicate the location of the soft palate muscles. Asterisks indicate defects of the LVP and PLP (H,J). TVP, tensor veli palatini; LVP, levator veli palatini; PLP, palatopharyngeus; PP, pterygoid plate. *n*=4. Scale bars: 500 µm in A,B; 1 mm in C,D; 250 µm in E-J.

interaction of Dlx5-positive CNC cells with myogenic cells at various stages of muscle development. In the TVP region of *Dlx5-Cre;tdTomato* mice, MyoD-positive muscle progenitor cells were detectable at E13.5 and E14.5, but fewer cells were detectable at E17.5 (Fig. 3A-C,S). MHC-positive muscle cells were detectable at E13.5 and in greater numbers at E14.5 and E17.5 (Fig. 3D-F,V). Thus, as MHC-positive muscle cells were increasing in number, MyoD-positive muscle progenitor cells were decreasing, indicating that our assays faithfully represent the myogenic differentiation program *in vivo*. Next, we compared the Dlx5 expression pattern with that of MyoD- and MHC-positive muscle cells. We found that Dlx5-positive cells were not immediately adjacent to the MyoD- and MHC-positive cells in the TVP region (Fig. 3A-F). Our results suggest that Dlx5-expressing CNC cells may not regulate TVP development.

Development (2017) 144, 4037-4045 doi:10.1242/dev.155176

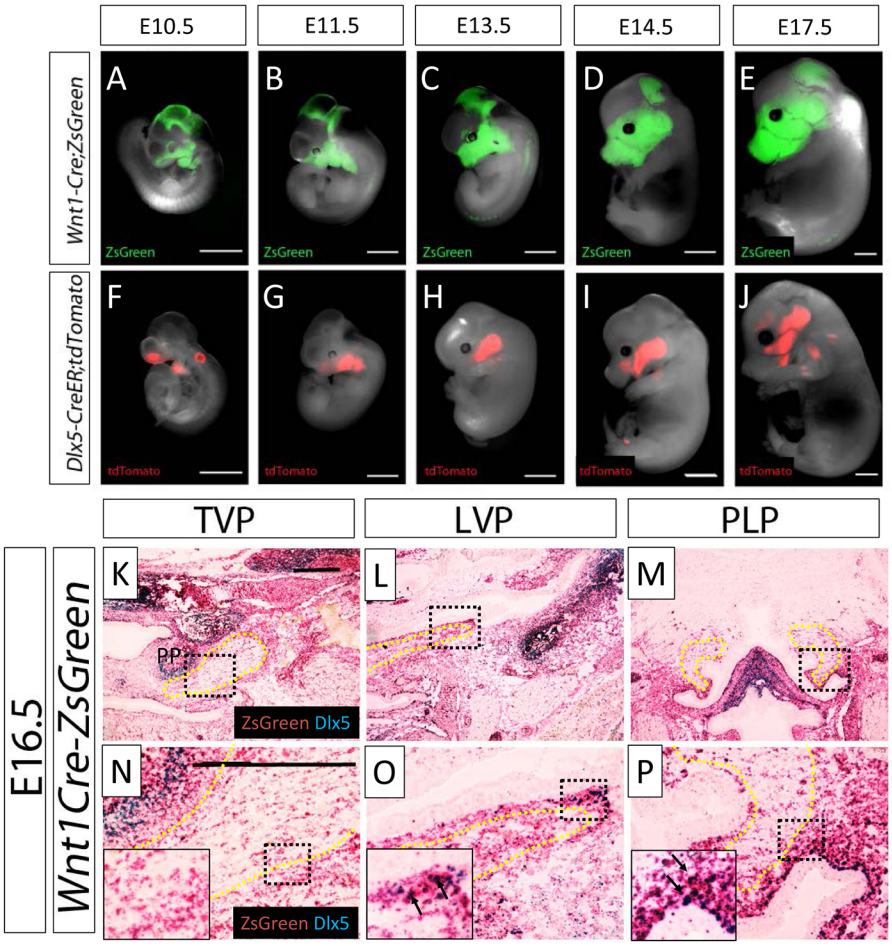

Fig. 2. Dlx5 is expressed by a subset of CNC-derived cells during soft palate development. (A-J) Whole-mount *Wnt1-Cre;ZsGreen* (green staining indicates CNC cells) and *Dlx5-CreER; tdTomato* (red staining indicates Dlx5 expression) embryos from E10.5 to E17.5. (K-P) RNAscope *in situ* hybridization analysis of Dlx5 (blue) and ZsGreen (red) in sections of E16.5 *Wnt1-Cre; ZsGreen* mice at the level of the TVP, LVP and PLP. Arrows represent colocalization of Dlx5 and ZsGreen signals in the LVP and PLP regions (O,P). (N-P) Magnified images of the areas outlined in K-M, respectively. Insets in N-P are magnifications of the regions outlined. Yellow dotted lines indicate the location of the TVP, LVP and PLP based on our previous report (Grimaldi et al., 2015). TVP, tensor veli palatini; LVP, levator veli palatini; PLP, palatopharyngeus; PP, pterygoid plate. *n*=3. Scale bars: 1 mm in A-J; 250 µm in K-P.

In the LVP and PLP regions, MyoD-positive muscle progenitor cells were detectable at E14.5 and E15.5 (Fig. 3G,H,M,N). These cells were decreased in number at E17.5 in the LVP region (Fig. 3I,T), but they persisted throughout the PLP from the lateral region to the midline (Fig. 3O,U). MHC-positive muscle cells were detectable at E14.5 and present in greater numbers at E15.5 and E17.5 (Fig. 3J-L,P-R,W,X). These data suggest that the differentiation of the PLP is not yet finished at E17.5 and that the PLP differentiates later than the TVP and LVP. Dlx5-positive CNC cells were immediately adjacent to the MyoD- and MHC-positive cells in the regions of the LVP and PLP (Fig. 3G-R). In addition, more Dlx5-positive cells adjacent to MyoD- and MHC-positive cells were detectable in the LVP and PLP compared with the TVP (Fig. 3Y-B′). These results indicate that Dlx5-positive CNC cells closely associate with muscle progenitor cells in the LVP and PLP, but not the TVP, regions, consistent with a role related to muscle development.

Cellular mechanisms of LVP and PLP defects resulting from loss of Dlx5

In order to examine the cellular defect of *Dlx5*$^{-/-}$ mice in greater detail, we analyzed when the soft palate muscles began to exhibit defects. In both the LVP and PLP regions, there was no significant difference between control and *Dlx5*$^{-/-}$ embryos at E13.5 (data not shown). *Dlx5*$^{-/-}$ embryos began to exhibit defects in the LVP region by E14.5 (Fig. S2A-F), after palatal shelf elevation, which persisted at E15.5 (Fig. S2G-L). After the PLP began to grow from the lateral region towards the midline, muscle defects were detectable in *Dlx5*$^{-/-}$ embryos at E15.5 (Fig. S2M-R). Next, we investigated the potential cellular mechanism for the defects in the LVP and PLP regions of *Dlx5*$^{-/-}$ mice by determining whether Dlx5 disruption affects apoptosis and proliferation. First, we compared expression of caspase 3 in control and *Dlx5*$^{-/-}$ mice for analysis of apoptosis. In the TVP region, apoptosis was unaffected in *Dlx5*$^{-/-}$ mice compared with control mice at E14.5 and E15.5 (Fig. 4A-D,M-P). In contrast, more caspase3-positive cells were detectable in *Dlx5*$^{-/-}$ mice compared with control mice at E14.5 and E15.5 in the LVP region (Fig. 4E-H). The apoptotic cells colocalized with MyoD-negative CNC cells at E14.5 and MyoD-positive muscle progenitor cells at E15.5 (Fig. 4G,H,Q-T). In the PLP region, loss of Dlx5 resulted in increased apoptosis in MyoD-negative CNC cells at E15.5 (Fig. 4J,L,V,X), but apoptosis was unaffected in CNC and muscle progenitor cells at E14.5 (Fig. 4I,K,U,W). These results demonstrate that loss of Dlx5 leads to increased apoptosis of CNC cells during early development of the soft palate in the LVP and PLP, but not the TVP. The earlier onset of apoptosis in CNC cells in the LVP at E14.5 versus E15.5 in the PLP is perhaps due to the earlier development of the LVP compared with the PLP (see Fig. 3). Moreover, the increased apoptosis switches from CNC cells to muscle progenitor cells during later development of the LVP.

Next, we compared expression of phospho-histone 3 in control and *Dlx5*$^{-/-}$ mice for analysis of proliferation. Robust proliferation was detectable in the LVP and PLP regions of E14.5 and E15.5 control mice, primarily in MyoD-negative CNC cells, whereas we detected decreased cell proliferation in *Dlx5*$^{-/-}$ mice (Fig. 5C,D,G, H,K,L,O,P). In contrast, cell proliferation in the TVP of *Dlx5*$^{-/-}$

Development (2017) 144, 4037-4045 doi:10.1242/dev.155176

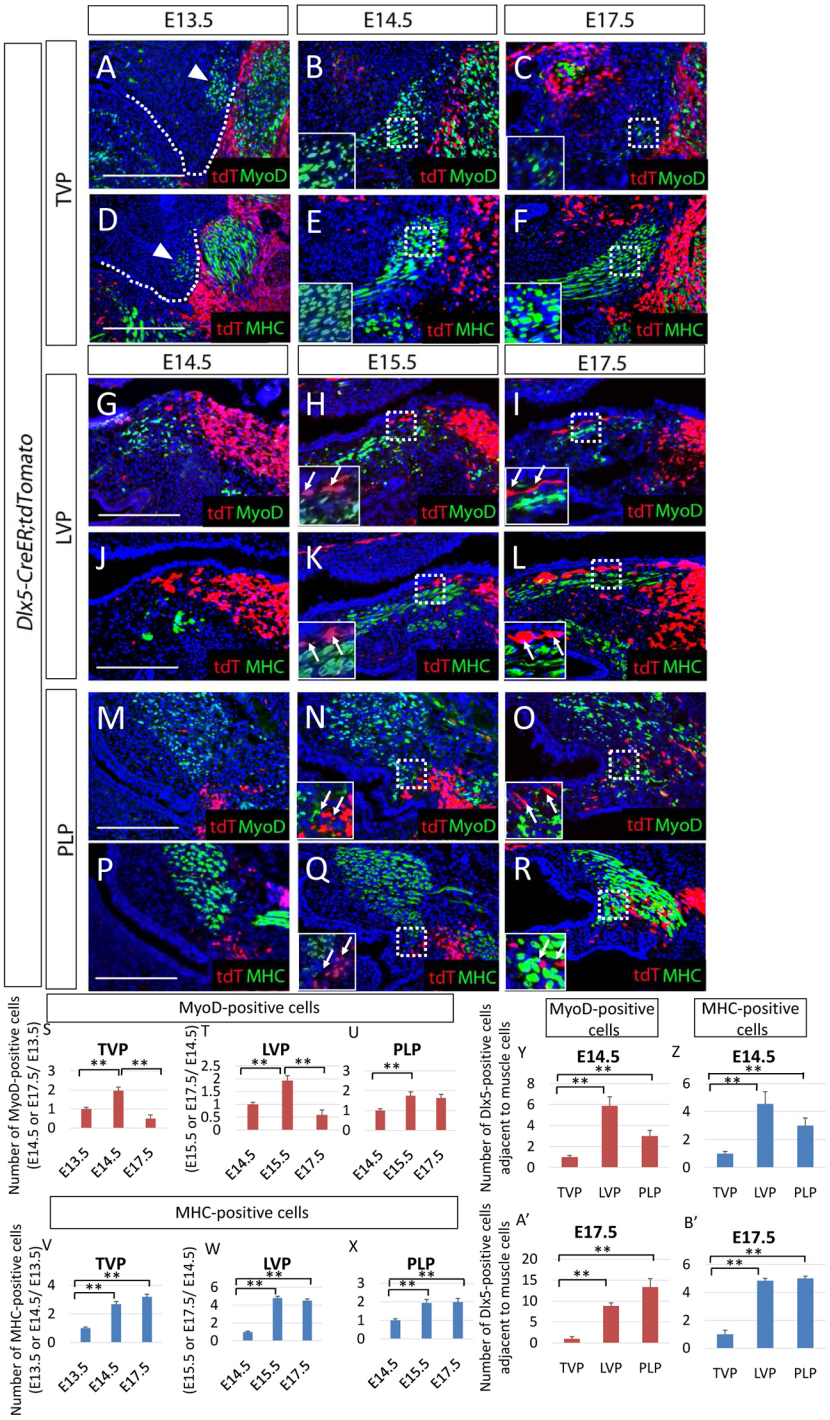

Fig. 3. Dlx5-positive CNC cells are adjacent to muscle progenitor cells in the LVP and PLP regions, but not the TVP region. (A-R) Visualization of tdTomato (tdT, red) and immunostaining of myoblast determination protein 1 (MyoD, green) or myosin heavy chain (MHC, green) in coronal sections of E13.5 to E17.5 *Dlx5-CreER;tdTomato* embryos at the level of the TVP (A-F), LVP (G-L) or PLP (M-R). White broken lines indicate palatal shelves and arrowheads indicate the differentiating TVP (A,D). White insets are magnified images of the boxed regions. Arrows indicate Dlx5-positive cells immediately adjacent to myogenic cells. (S-X) Quantification of MyoD-positive (S-U) and MHC-positive (V-X) cells in the TVP, LVP and PLP regions. (Y-B′) Quantification of Dlx5-positive cells adjacent to MyoD-positive (Y,A′) and MHC-positive (Z,B′) cells in the TVP, LVP and PLP regions at E14.5 and E17.5. Results are presented as the ratio of Dlx5-positive cells near the LVP or PLP (with no blue cells between green and red cells) compared with those near the TVP. Three samples per genotype were analyzed. $^{**}P<0.01$, $n=3$. Data are mean± s.e.m. TVP, tensor veli palatini; LVP, levator veli palatini; PLP, palatopharyngeus. Scale bars: 250 µm.

mice was indistinguishable from that of control mice (Fig. 5A,B,E, F,I,J,M,N). These results suggest that Dlx5-mediated signaling in CNC cells may be crucial for the proliferation of CNC cells and the survival of muscle progenitor and CNC cells in the LVP and PLP regions of the soft palate, but not in the TVP region.

Dlx5 controls Fgf10 signaling to regulate soft palate muscle development

In order to analyze the molecular mechanism of muscle development in the LVP and PLP, we performed RNA profile analysis using the samples from soft palate tissues of E14.5 control and *Dlx5*$^{-/-}$ embryos. In this comparison, we found 674 genes differentially expressed (≥1.7-fold, FDR $P<0.05$, $n=3$), 416 of them downregulated and 258 upregulated in *Dlx5*$^{-/-}$ mice.

We focused on FGF signaling, one of the differentially expressed signaling pathways we identified from the RNA profile analysis (Fig. S3). Previous studies have reported that many FGF family members are expressed in the skeletal muscles (Hannon et al., 1996; Hébert et al., 1990). Moreover, our group found that TGFβ-mediated FGF10 signaling in neural crest cells controls the development of muscle progenitor cells during tongue morphogenesis (Hosokawa et al., 2010). Thus, we first analyzed gene expression of *Fgf10* in the soft palate region using *in situ* hybridization analysis. *Fgf10* expression was detectable in the TVP of both control and *Dlx5*$^{-/-}$

Development (2017) 144, 4037-4045 doi:10.1242/dev.155176

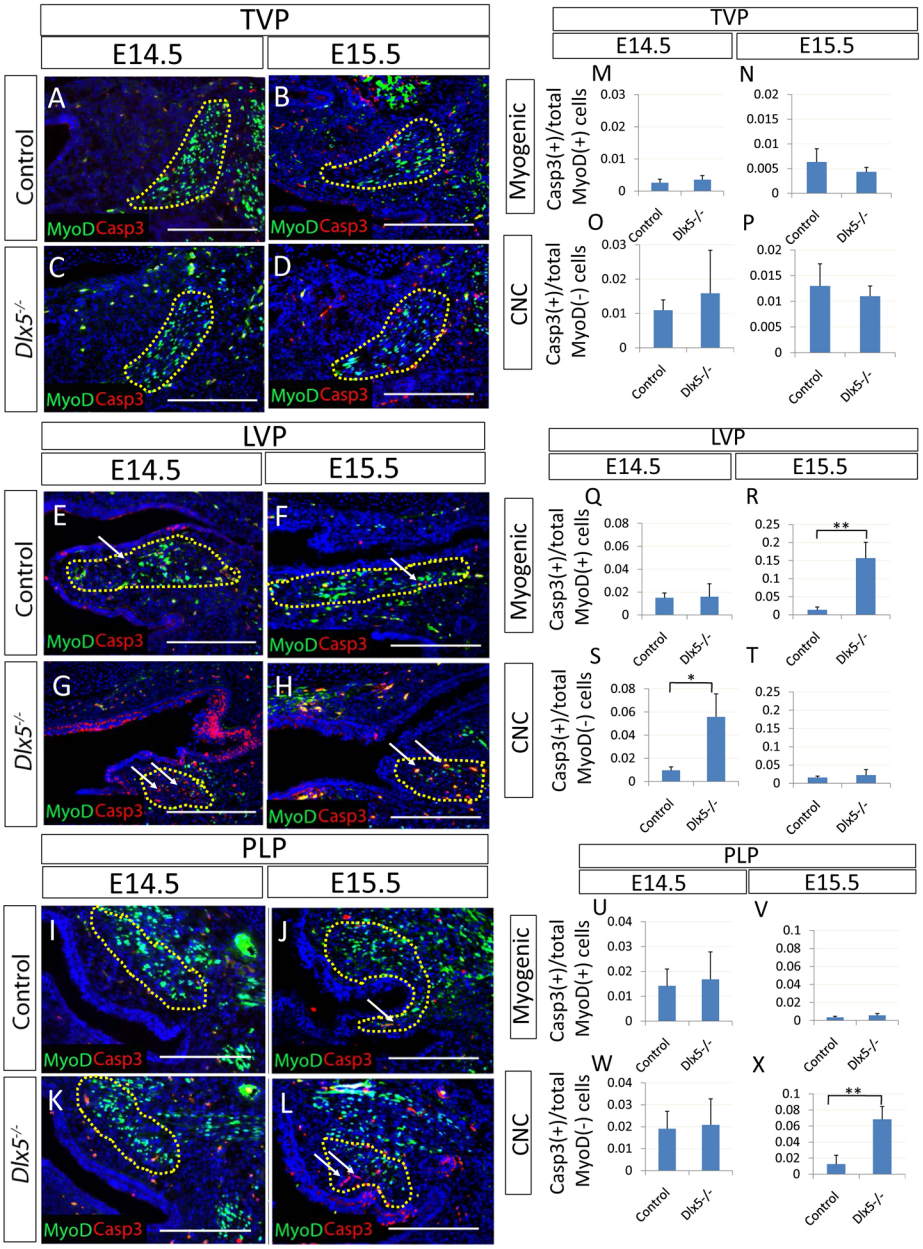

Fig. 4. Loss of Dlx5 results in increased apoptosis in both CNC and muscle progenitor cells of the LVP and PLP. (A-L) Immunostaining of active caspase 3 (Casp3, red) and myoblast determination protein 1 (MyoD, green) in control and *Dlx5*$^{-/-}$ embryos at the level of the TVP (A-D), LVP (E-H) and PLP (I-L) at E14.5 and E15.5. Yellow dotted lines indicate the location of the soft palate muscles based on MyoD-positive muscle progenitor cells in Fig. S2 and our previous report (Grimaldi et al., 2015). Arrows indicate apoptotic cells. (M-X) Quantification of apoptosis in MyoD-positive muscle progenitor cells (myogenic) and MyoD-negative CNC cells (CNC) from control and *Dlx5*$^{-/-}$ embryos in the TVP (M-P), LVP (Q-T) and PLP (U-X) regions (within the yellow dotted lines). Three samples per genotype were analyzed. $^{**}P<0.01$, $^{*}P<0.05$, $n=3$. Data are mean±s.e.m. TVP, tensor veli palatini; LVP, levator veli palatini; PLP, palatopharyngeus. Scale bars: 250 µm.

mice (Fig. 6A,D). In the LVP and PLP regions, *Fgf10* expression was detectable in control mice but was decreased in *Dlx5*$^{-/-}$ mice (Fig. 6B,C,E,F). We confirmed that *Fgf10* expression was decreased in the soft palate region using quantitative PCR (Fig. S4). Based on this, we analyzed whether activation of FGF10 signaling could rescue the development of the soft palate muscles in *Dlx5*$^{-/-}$ mice. We cultured cells from the soft palate tissues of E13.5 control and *Dlx5*$^{-/-}$ mice treated with or without exogenous FGF10 for 1 week and analyzed muscle differentiation by counting MHC-positive cells per DAPI-positive total cells. Consistent with our results above, more MHC-positive cells were detectable in mock-treated control cells than *Dlx5*$^{-/-}$ cells (Fig. 7A,C,I). After treatment of *Dlx5*$^{-/-}$ cells with FGF10, the number of MHC-positive cells increased and was similar to that of control cells (Fig. 7A-D,I). These results suggest that loss of Dlx5 affects muscle development of the LVP and PLP via regulation of FGF10 signaling. We also analyzed whether activation of FGF10 signaling can rescue proliferative ability in the soft palate of *Dlx5*$^{-/-}$ mice. We cultured cells from the soft palate tissues of E13.5 control and *Dlx5*$^{-/-}$ mice treated with or without FGF10 for 2 days and analyzed their proliferative ability. More MyoD-negative CNC cells were proliferating in control samples than in *Dlx5*$^{-/-}$ samples (Fig. 7E,G,J), and total proliferation was also decreased in *Dlx5*$^{-/-}$ cells (Fig. S5). After treatment of *Dlx5*$^{-/-}$ cells with FGF10, the number of proliferative CNC cells increased in the *Dlx5*$^{-/-}$ samples and was similar to that of control cells (Fig. 7E-H,J). These results suggest that loss of Dlx5 affects proliferative ability of CNC cells via regulation of FGF10 signaling.

DISCUSSION

Dlx5 is crucial for oropharyngeal patterning and soft palate muscles derived from the 4th PA

In this study, we found that loss of Dlx5 led to defects in oropharyngeal patterning and soft palate muscles derived from the 4th pharyngeal arch (PA). During the formation of the head muscles, the precursors of the pharyngeal mesoderm, which is a subset of the head mesoderm that surrounds the developing

Development (2017) 144, 4037-4045 doi:10.1242/dev.155176

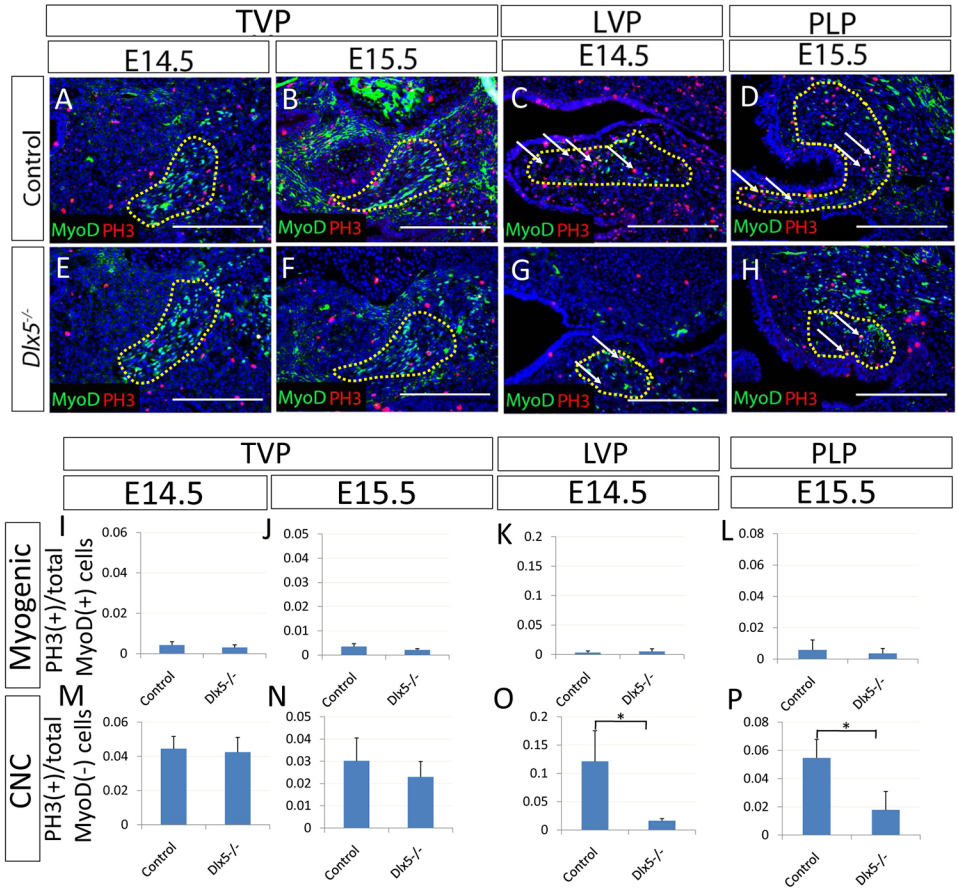

Fig. 5. Loss of Dlx5 results in reduced proliferation of CNC cells in the LVP and PLP regions. (A-H) Immunostaining of active phosphohistone 3 (PH3, red) and myoblast determination protein 1 (MyoD, green) in sections of control and *Dlx5*$^{-/-}$ embryos at E14.5 and E15.5 at the level of the TVP (A,B,E,F), at E14.5 at the level of the LVP (C,G) and at E15.5 at the level of the PLP (D,H). Yellow dotted lines indicate the location of the soft palate muscles based on MyoD-positive muscle progenitor cells in Fig. S2 and on our previous report (Grimaldi et al., 2015). Arrows indicate proliferative cells. (I-P) Quantification of proliferation in MyoD-positive muscle progenitor cells (myogenic) and MyoD-negative CNC cells (CNC) from control and *Dlx5*$^{-/-}$ embryos in the TVP, LVP and PLP regions (within the yellow dotted lines). Three samples per genotype were analyzed. **P*<0.05, *n*=3. Data are mean±s.e.m. TVP, tensor veli palatini; LVP, levator veli palatini; PLP, palatopharyngeus. Scale bars: 250 µm.

pharynx, stream into the neighboring PAs that form the templates of the craniofacial structures. In the soft palate, the TVP is derived from the 1st PA, whereas the LVP, PLP and PLG are derived from the 4th PA (Lieberman, 2011). Muscles derived from different PAs must be physically and functionally integrated. For example, muscles for facial expression that are derived from the 2nd PA and muscles for mastication that are derived from the 1st PA work together. These muscles are highly diverse and reflect evolutionary changes related to sites of jaw articulation and modes of masticatory movement (Noden and Francis-West, 2006). Moreover, many factors contribute to the development of muscles from specific PAs. Tbx1 is expressed in the premyogenic mesoderm of the 1st and 2nd Pas, and affects the maturation of the PA myoblasts and formation of some head muscles (Kelly et al., 2004). Pitx2 is expressed in the 1st PA mesoderm at E9.5 and co-expressed with Tbx1 and MyoD in the 1st and 2nd PAs at E10.5 (Shih et al., 2008). Previous studies have demonstrated that Pitx2 specifies 1st PA-derived muscles through regulating the activation of Tbx1 (Shih et al., 2007). However, the factors that affect muscle development from other PAs remain unclear. In this study, loss of Dlx5 led to defects of the LVP, PLP, PLG and superior pharyngeal constrictor, which are all derived from the 4th PA, whereas the TVP, which is derived from the 1st PA, was unaffected. These results suggest that Dlx5 plays a crucial role in the development of muscles derived from the 4th PA.

Previous studies have shown that there is significant molecular heterogeneity in the regulation of head muscle development (Nathan et al., 2008). In chick embryos, the pharyngeal mesoderm can be subdivided into groups of cells based on their

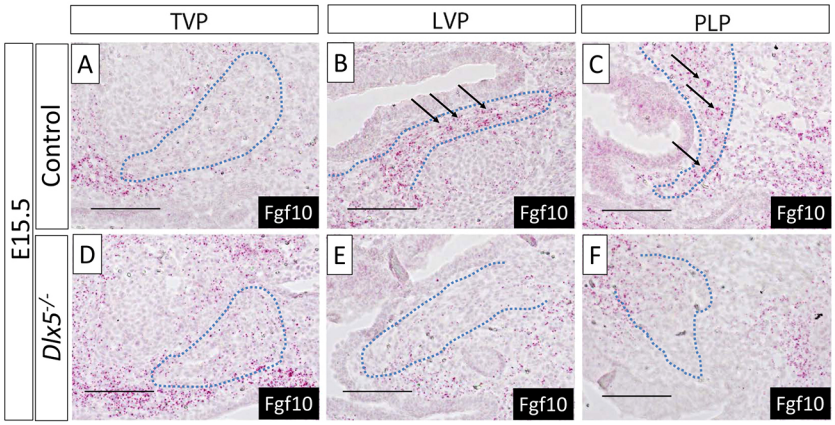

Fig. 6. Loss of Dlx5 results in downregulated *Fgf10* expression in the LVP and PLP regions. (A-F) RNAscope *in situ* hybridization analysis of *Fgf10* in sections of E15.5 control and *Dlx5*$^{-/-}$ embryos at the level of the TVP, LVP and PLP. Red dots represent positive signal of *Fgf10* indicated by arrows. Blue dotted lines indicate the location of the TVP, LVP and PLP based on MHC-positive cells and our previous report (Grimaldi et al., 2015). TVP, tensor veli palatini; LVP, levator veli palatini; PLP, palatopharyngeus. *n*=3. Scale bars: 500 µm.

Development (2017) 144, 4037-4045 doi:10.1242/dev.155176

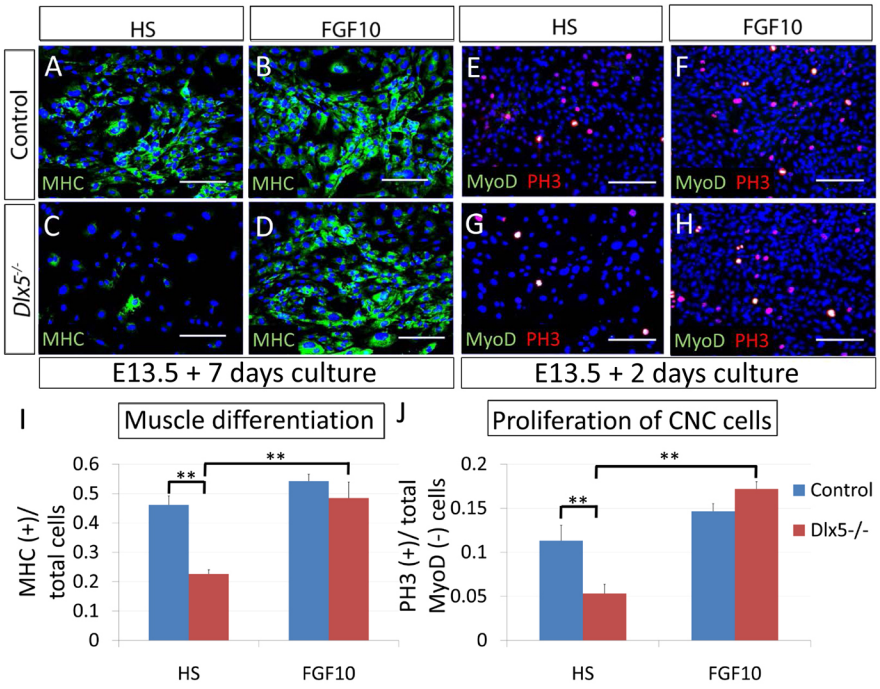

Fig. 7. Activation of FGF10 signaling rescues differentiation of muscle progenitor cells and proliferation of CNC cells in *Dlx5*$^{-/-}$ mice. (A-D) Immunostaining of myosin heavy chain (MHC, green) in cells from the soft palates of E13.5 control and *Dlx5*$^{-/-}$ embryos cultured with 2% horse serum (HS) or 2% HS+10 ng/ml FGF10 for 1 week. (E-H) Immunostaining of active phosphohistone 3 (PH3, red) and myoblast determination protein 1 (MyoD, green) in cells from the soft palate of E13.5 control and *Dlx5*$^{-/-}$ embryos cultured with 2% horse serum (HS) or 2% HS+10 ng/ml FGF10 for 2 days. (I,J) Quantification of MHC-positive muscle cells from A-D and PH3-positive CNC cells from E-H. Three samples per genotype were analyzed. $^{**}P<0.01$, $n=3$. Data are mean±s.e.m. Scale bars: 250 µm.

contribution to muscle development associated with different pharyngeal arches (Michailovici et al., 2015). However, there is not yet any definitive information that links specific molecular regulators with the development of muscles within each pharyngeal arch. In this study, the discovery that Dlx5 is specifically associated with muscles derived from the 4th pharyngeal arch in mammals highlights the early establishment of arch identity during head muscle development. It also begins to provide unique tools for us to target pharyngeal arch-specific derivatives in order to investigate the regulatory mechanisms for craniofacial development.

Dlx5-positive CNC cells guide migration of muscle progenitor cells derived from the 4th PA

CNC cells play a crucial role in the patterning of the head muscles (Olsson et al., 2001; Schilling and Kimmel, 1997). Previous studies have demonstrated that ablation of CNC cells in chick embryos leads to abnormal migratory pathways and anterior-posterior registration of the mesoderm cells (Rinon et al., 2007). Our previous study showed that CNC-derived cells control muscle development in the tongue through tissue-tissue interactions (Hosokawa et al., 2010). In the soft palate region, CNC-derived cells migrate into the primordium of the soft palate and form a scaffold to guide the migration of myogenic progenitors (Grimaldi et al., 2015). In this study, we demonstrated that Dlx5-positive cells are a subset of CNC-derived cells and that Dlx5-positive CNC cells are adjacent to myogenic cells in the LVP and PLP regions. Earlier in development, Dlx5-positive cells were detectable in the olfactory placode, otic placode and PAs. These patterns are consistent with the results of previous gene expression analyses using *in situ* hybridization (Depew et al., 1999). Strikingly, Dlx5-positive CNC cells are not adjacent to myogenic cells in the TVP region, which is derived from the 1st PA and appears unaffected in *Dlx5*$^{-/-}$ mice. These results suggest that Dlx5-positive CNC cells have a close association with myogenic cells and guide migration of myogenic cells to the terminal differentiation site only in muscles derived from the 4th PA.

CNC cells give rise to all facial bone and some of the calvaria. Head muscles attach to these bones through tendons, which are also CNC-derived tissue (Grenier et al., 2009; Han et al., 2012). Previous studies have shown that CNC cells are progressively involved in patterning and development of head muscles (Tzahor, 2015). As pharyngeal mesodermal progenitors migrate into the pharyngeal arch, they also encounter signals from pharyngeal ectoderm and endoderm. In order to investigate the specific roles of CNC cells in regulating head muscle development, we need to identify cell type-specific regulatory factors and test their instructive role in regulating head muscle development. Clearly, the Dlx5-mediated signaling network is crucial for CNC and myogenic progenitor interactions during the development of 4th pharyngeal arch muscles.

Dlx5-mediated signaling in CNC cells regulates the fate of CNC and muscle progenitor cells derived from the 4th PA

In the PAs, CNC cells that surround the muscle anlagen separate the myoblasts from the overlying surface ectoderm. Subsequently, the muscle progenitors within the PAs differentiate and form each of the muscles (Michailovici et al., 2015). Studies have reported that CNC cells are not essential for early myogenic development, but are necessary for the migration, positioning and differentiation of cranial muscle precursors in vertebrates (Rinon et al., 2007). Previously, our work revealed that Dlx5 controls the fate of CNC cells in the anterior palate region (Han et al., 2009). In this study, we discovered that loss of Dlx5 leads to reduced cell proliferation and increased apoptosis in CNC cells at earlier stages and increased apoptosis in myogenic cells at later stages. In addition to CNC cells, palatal epithelial signals can also affect muscle development through tissue-tissue interactions. For example, epithelial TGFβ signaling can regulate WNT signaling activity in the soft palate mesenchyme and affect muscle development (Iwata et al., 2014). Members of the TGFβ family have been shown to act both upstream and downstream of Dlx5 in regulating the fate of CNC cells during craniofacial development. Our results indicate that Dlx5-mediated signaling affects proliferation and apoptosis of CNC cells. Furthermore, myogenic progenitor cells fail to migrate correctly and myogenic cell survival is affected secondarily in Dlx5 mutant mice. It will be crucial to identify the signaling molecules regulated

Development (2017) 144, 4037-4045 doi:10.1242/dev.155176

by Dlx5 that can exert action on myogenic progenitors during soft palate muscle development.

FGF10 signaling pathway may mediate Dlx5 activity in muscles derived from the 4th PA

We identified the FGF pathway as altered in *Dlx5*$^{-/-}$ mice based on RNA-seq analysis. Many members of the FGF signaling family are expressed in muscle cells (Hannon et al., 1996), and the TGFβ-induced FGF10 signaling pathway plays crucial roles in muscle development of the tongue (Hosokawa et al., 2010). In addition, FGF7 and FGF10 are expressed in the anterior palate region, and *Fgfr2b*$^{-/-}$ and *Ffg10*$^{-/-}$ mice exhibit cleft palate (Rice et al., 2004). During palatogenesis, Dlx-regulated FGF7 signaling inhibits the expression of Shh, which in turn controls the fate of CNC cells through tissue-tissue interaction (Han et al., 2009). In this study, we found that expression of FGF10 is decreased in *Dlx5*$^{-/-}$ mice in soft palate muscles derived from the 4th PA. In addition, activation of FGF10 signaling rescued the differentiation program of myogenic cells and proliferative ability of CNC cells in *Dlx5*$^{-/-}$ mice. These results clearly indicate that a Dlx5/FGF signaling interaction plays a key role in patterning and development of the hard and soft palate. Previous studies have shown that key transcription factors expressed in CNC cells may regulate FGF signaling to control craniofacial and cardiac development. For example, neural crest cell ablation in the Hox-negative mid-diencephalon through the rhombomere 2 region led to downregulation of FGF8 expression and abnormal pharyngeal arch development in chick embryos (Creuzet et al., 2004). On the other hand, Hox-positive cardiac neural crest cells appear to inhibit FGF8 signaling (Michailovici et al., 2015). Although more work is need to elucidate the precise mechanism by which neural crest cells regulate FGF signaling, it appears to be a crucial and well-conserved mechanism in mediating tissue-tissue interactions during embryonic development.

In summary, we have found that Dlx5-mediated FGF10 signaling plays a crucial role in oropharyngeal patterning and the development of muscles derived from 4th PA through interactions between CNC and muscle progenitor cells. These findings are important for clinical studies that aim to correct soft palate muscle development defects. Moreover, the mechanisms of soft palate muscle development identified in this study may lead to a better approach to muscle regeneration in individuals with soft palate muscle defects in the future.

MATERIALS AND METHODS

Animals

To generate *Dlx5*$^{-/-}$ mice, we mated *Dlx5*$^{+/-}$ with *Dlx5*$^{+/-}$ mice. To generate *Wnt1-Cre;ZsGreen* mice, we mated *Wnt1-Cre;ZsGreen*$^{fl/+}$ males with *ZsGreen*$^{fl/fl}$ females. To generate *Dlx5-CreER;tdTomato* mice, we mated *Dlx5-CreER;tdTomato*$^{fl/+}$ males with *tdTomato*$^{fl/fl}$ females. Pregnant females were harvested based on staging determined by counting the days after detection of a vaginal plug and Theiler staging criteria (Theiler, 1989). The animals were euthanized through carbon dioxide overdose followed by cervical dislocation. All studies were performed with the approval of the Institutional Animal Care and Use Committee (IACUC) of the University of Southern California.

MicroCT analysis

For microCT analysis, we used a SCANCO μCT50 device at the University of Southern California Molecular Imaging Center. The images were detected with the X-ray source at 70 kVp and 114 μA. The data were collected at a resolution of 10 μm. 3D reconstruction was performed using AVIZO 7.1 (Visualization Sciences Group).

Tamoxifen injection

Tamoxifen (Sigma, T5648) was dissolved in corn oil (Sigma, C8267) at 20 mg/ml and injected intraperitoneally 2 days before sacrificing mice (single injection, 2 mg/10 g body weight).

Histological analysis

For Hematoxylin and Eosin staining, samples were fixed in 4% paraformaldehyde (PFA) and decalcified with 10% EDTA. Next, samples were dehydrated with serial ethanol and embedded in paraffin wax. Sections were cut at 7 μm and Hematoxylin and Eosin staining was performed using standard procedures. For immunofluorescence staining, the following primary antibodies were used: myoblast determination protein 1 (MyoD; DAKO, M3512; 1:50), myosin heavy chain (MHC; DSHB, P13538; 1:10), active caspase 3 (Casp3; Abcam, ab2302; 1:100), phosphohistone H3 (PH3; Millipore, 06-570; 1:100) and RFP (tdTomato; Rockland, 600-401-379; 1:200). Alexa Fluor 488 and 568 were used as secondary antibodies. Staining procedure was performed according to standard protocol (Iwata et al., 2012; Sugii et al., 2014). Sections were counterstained with DAPI and imaged by Leica DMI 3000B and Keyence BZ-X710 microscopes.

RNAscope *in situ* hybridization

Soft palate tissue was collected at E15.5 and E16.5, and fixed in fresh 4% PFA. Samples were passed through 15% and 30% sucrose and embedded in OCT compound (Tissue-Tek). Sections were cut at 7 μm and staining was performed with the RNAscope 2.5HD Reagent Kit-RED assay (Advanced Cell Diagnostics, 322350) according to the manufacturer's protocol. The RNAscope probes used in this study were Fgf10 (Advanced Cell Diagnostics, 446371), Dlx5 (Advanced Cell Diagnostics, 478151) and ZsGreen (Advanced Cell Diagnostics, 461251-C2).

RNA sequencing

Samples from the soft palate tissue of E14.5 *Dlx5*$^{-/-}$ and control mice were used to extract total RNA. cDNA library preparation and sequencing were performed at the USC Molecular Genomics Core. A total of 400 million paired-end reads with 75 cycles were performed on Illumina Next Seq 500 equipment for three pairs of samples. Raw reads were trimmed, aligned using TopHat2 with mm 10 genomes and normalized using RPKM. Differential expression was calculated by selecting transcripts that changed with a significance of $P<0.05$.

Quantitative RT-PCR

Total RNA was isolated from mouse soft palate tissue dissected at E13.5 using QIAshredder and RNeasy Micro extraction kits (Qiagen) as described previously (Iwata et al., 2010). The following PCR primers were used: *Fgf10*, 5′-TTTGGTGTCTTCGTTCCCTGT-3′ and 5′-TAGCTCCGCAC-ATGCCTTC-3′.

Cell culture

Soft palate tissue was dissected from control and *Dlx5*$^{-/-}$ embryos at E13.5, followed by treatment with 2.4 U/ml Dispase I (Roche Applied Science) for 1 h at 37°C. The cells were isolated and cultured as previously described (Hosokawa et al., 2010). Where indicated, mouse recombinant FGF10 (10 ng/ml; R&D) was added to the medium after plating and re-added every other day, followed by cell culture for 2 days or 1 week.

Statistical analysis

Two-tailed Student's *t*-tests were applied for statistical analysis. For all graphs, data are mean±s.d. $P<0.05$ was considered statistically significant.

Acknowledgements

We are grateful to Dr Julie Mayo and Dr Bridget Samuels for critical reading and editing of the manuscript. We thank Dr John Rubenstein at UCSF for *Dlx5* mutant mice, Vasu Punj for analyses of RNA-seq and USC Norris Medical Library Bioinformatics Service for assisting with data analysis. The bioinformatics software and computing resources used in the analysis are funded by USC Office of Research and the Norris Medical Library.

Competing interests

The authors declare no competing or financial interests.

Author contributions

Conceptualization: H.S., Y.C.; Methodology: H.S., J.L., C.P., T.V.-H., J.F., Y.G., Y.C.; Software: T.V.-H., Y.C.; Validation: H.S., C.P., T.V.-H., J.F., J.J., Y.Y., Y.G., Y.C.; Formal

analysis: H.S., A.G., J.L., C.P., J.F., Y.G., Y.C.; Investigation: H.S., J.L., Y.Y., Y.C.; Resources: H.M., Y.C.; Data curation: H.S., A.G., J.L., C.P., J.J., Y.Y., Y.C.; Writing - original draft: H.S., Y.C.; Writing - review & editing: Y.C.; Visualization: J.J., Y.C.; Supervision: H.S., H.M., Y.C.; Project administration: H.S., Y.C.; Funding acquisition: H.M., Y.C.

Funding

This work was supported by the National Institute of Dental and Craniofacial Research (National Institutes of Health) (R37 DE012711 and U01 DE024421 to Y.C.). Deposited in PMC for release after 12 months.

Data availability

RNA sequencing data are available at Gene Expression Omnibus with accession number GSE104163.

Supplementary information

Supplementary information available online at
http://dev.biologists.org/lookup/doi/10.1242/dev.155176.supplemental

References

Barron, F., Woods, C., Kuhn, K., Bishop, J., Howard, M. J. and Clouthier, D. E. (2011). Downregulation of Dlx5 and Dlx6 expression by Hand2 is essential for initiation of tongue morphogenesis. *Development* **138**, 2249-2259.

Carvajal Monroy, P. L., Grefte, S., Kuijpers-Jagtman, A. M., Wagener, F. A. and Von den Hoff, J. W. (2012). Strategies to improve regeneration of the soft palate muscles after cleft palate repair. *Tissue Eng. Part B Rev.* **18**, 468-477.

Chanoine, C., Guyot-Lenfant, M., Saadi, A., Perasso, F., Salles-Mourlan, A. M. and Gallien, C. L. (1990). Myosin structure and thyroidian control of myosin synthesis in urodelan amphibian skeletal muscle. *Int. J. Dev. Biol.* **34**, 163-170.

Creuzet, S., Schuler, B., Couly, G. and Le Douarin, N. M. (2004). Reciprocal relationships between Fgf8 and neural crest cells in facial and forebrain development. *Proc. Natl. Acad. Sci. USA* **101**, 4843-4847.

Depew, M. J., Liu, J. K., Long, J. E., Presley, R., Meneses, J. J., Pedersen, R. A. and Rubenstein, J. L. (1999). Dlx5 regulates regional development of the branchial arches and sensory capsules. *Development* **126**, 3831-3846.

Depew, M. J., Lufkin, T. and Rubenstein, J. L. (2002). Specification of jaw subdivisions by Dlx genes. *Science* **298**, 381-385.

Evans, A., Ackermann, B. and Driscoll, T. (2010). Functional anatomy of the soft palate applied to wind playing. *Med. Probl. Perform. Art.* **25**, 183-189.

Grenier, J., Teillet, M.-A., Grifone, R., Kelly, R. G. and Duprez, D. (2009). Relationship between neural crest cells and cranial mesoderm during head muscle development. *PLoS ONE* **4**, e4381.

Grimaldi, A., Parada, C. and Chai, Y. (2015). A comprehensive study of soft palate development in mice. *PLoS ONE* **10**, e0145018.

Han, J., Mayo, J., Xu, X., Li, J., Bringas, P., Jr, Maas, R. L., Rubenstein, J. L. R. and Chai, Y. (2009). Indirect modulation of Shh signaling by Dlx5 affects the oral-nasal patterning of palate and rescues cleft palate in Msx1-null mice. *Development* **136**, 4225-4233.

Han, D., Zhao, H., Parada, C., Hacia, J. G., Bringas, P., Jr and Chai, Y. (2012). A TGFbeta-Smad4-Fgf6 signaling cascade controls myogenic differentiation and myoblast fusion during tongue development. *Development* **139**, 1640-1650.

Hannon, K., Kudla, A. J., McAvoy, M. J., Clase, K. L. and Olwin, B. B. (1996). Differentially expressed fibroblast growth factors regulate skeletal muscle development through autocrine and paracrine mechanisms. *J. Cell Biol.* **132**, 1151-1159.

Hébert, J. M., Basilico, C., Goldfarb, M., Haub, O. and Martin, G. R. (1990). Isolation of cDNAs encoding four mouse FGF family members and characterization of their expression patterns during embryogenesis. *Dev. Biol.* **138**, 454-463.

Hosokawa, R., Oka, K., Yamaza, T., Iwata, J., Urata, M., Xu, X., Bringas, P., Jr, Nonaka, K. and Chai, Y. (2010). TGF-beta mediated FGF10 signaling in cranial neural crest cells controls development of myogenic progenitor cells through tissue-tissue interactions during tongue morphogenesis. *Dev. Biol.* **341**, 186-195.

Iwata, J., Hosokawa, R., Sanchez-Lara, P. A., Urata, M., Slavkin, H. and Chai, Y. (2010). Transforming growth factor-beta regulates basal transcriptional regulatory machinery to control cell proliferation and differentiation in cranial neural crest-derived osteoprogenitor cells. *J. Biol. Chem.* **285**, 4975-4982.

Iwata, J., Hacia, J. G., Suzuki, A., Sanchez-Lara, P. A., Urata, M. and Chai, Y. (2012). Modulation of noncanonical TGF-beta signaling prevents cleft palate in Tgfbr2 mutant mice. *J. Clin. Invest.* **122**, 873-885.

Iwata, J., Suzuki, A., Yokota, T., Ho, T.-V., Pelikan, R., Urata, M., Sanchez-Lara, P. A. and Chai, Y. (2014). TGFbeta regulates epithelial-mesenchymal interactions through WNT signaling activity to control muscle development in the soft palate. *Development* **141**, 909-917.

Kelly, R. G., Jerome-Majewska, L. A. and Papaioannou, V. E. (2004). The del22q11.2 candidate gene Tbx1 regulates branchiomeric myogenesis. *Hum. Mol. Genet.* **13**, 2829-2840.

Lieberman, D. (2011). *The Evolution of the Human Head*. Cambridge, MA: Belknap Press of Harvard University Press.

Michailovici, I., Eigler, T. and Tzahor, E. (2015). Craniofacial muscle development. *Curr. Top. Dev. Biol.* **115**, 3-30.

Nathan, E., Monovich, A., Tirosh-Finkel, L., Harrelson, Z., Rousso, T., Rinon, A., Harel, I., Evans, S. M. and Tzahor, E. (2008). The contribution of Islet1-expressing splanchnic mesoderm cells to distinct branchiomeric muscles reveals significant heterogeneity in head muscle development. *Development* **135**, 647-657.

Noden, D. M. and Francis-West, P. (2006). The differentiation and morphogenesis of craniofacial muscles. *Dev. Dyn.* **235**, 1194-1218.

Olsson, L., Falck, P., Lopez, K., Cobb, J. and Hanken, J. (2001). Cranial neural crest cells contribute to connective tissue in cranial muscles in the anuran amphibian, Bombina orientalis. *Dev. Biol.* **237**, 354-367.

Parada, C., Han, D. and Chai, Y. (2012). Molecular and cellular regulatory mechanisms of tongue myogenesis. *J. Dent. Res.* **91**, 528-535.

Precious, D. S. and Delaire, J. (1993). Clinical observations of cleft lip and palate. *Oral Surg. Oral Med. Oral Pathol.* **75**, 141-151.

Rice, R., Spencer-Dene, B., Connor, E. C., Gritli-Linde, A., McMahon, A. P., Dickson, C., Thesleff, I. and Rice, D. P. C. (2004). Disruption of Fgf10/Fgfr2b-coordinated epithelial-mesenchymal interactions causes cleft palate. *J. Clin. Invest.* **113**, 1692-1700.

Rinon, A., Lazar, S., Marshall, H., Buchmann-Moller, S., Neufeld, A., Elhanany-Tamir, H., Taketo, M. M., Sommer, L., Krumlauf, R. and Tzahor, E. (2007). Cranial neural crest cells regulate head muscle patterning and differentiation during vertebrate embryogenesis. *Development* **134**, 3065-3075.

Robledo, R. F. and Lufkin, T. (2006). Dlx5 and Dlx6 homeobox genes are required for specification of the mammalian vestibular apparatus. *Genesis* **44**, 425-437.

Rudnicki, M. A., Schnegelsberg, P. N. J., Stead, R. H., Braun, T., Arnold, H.-H. and Jaenisch, R. (1993). MyoD or Myf-5 is required for the formation of skeletal muscle. *Cell* **75**, 1351-1359.

Schilling, T. F. and Kimmel, C. B. (1997). Musculoskeletal patterning in the pharyngeal segments of the zebrafish embryo. *Development* **124**, 2945-2960.

Shih, H. P., Gross, M. K. and Kioussi, C. (2007). Cranial muscle defects of Pitx2 mutants result from specification defects in the first branchial arch. *Proc. Natl. Acad. Sci. USA* **104**, 5907-5912.

Shih, H. P., Gross, M. K. and Kioussi, C. (2008). Muscle development: forming the head and trunk muscles. *Acta Histochem.* **110**, 97-108.

Sugii, H., Maeda, H., Tomokiyo, A., Yamamoto, N., Wada, N., Koori, K., Hasegawa, D., Hamano, S., Yuda, A., Monnouchi, S. et al. (2014). Effects of Activin A on the phenotypic properties of human periodontal ligament cells. *Bone* **66**, 62-71.

Theiler, K. (1989). *The House Mouse: Atlas of Embryonic Development*. New York: Springer.

Tzahor, E. (2015). Head muscle development. *Results Probl. Cell Differ.* **56**, 123-142.

SUPPLEMENTARY MATERIAL

Supplementary Figures

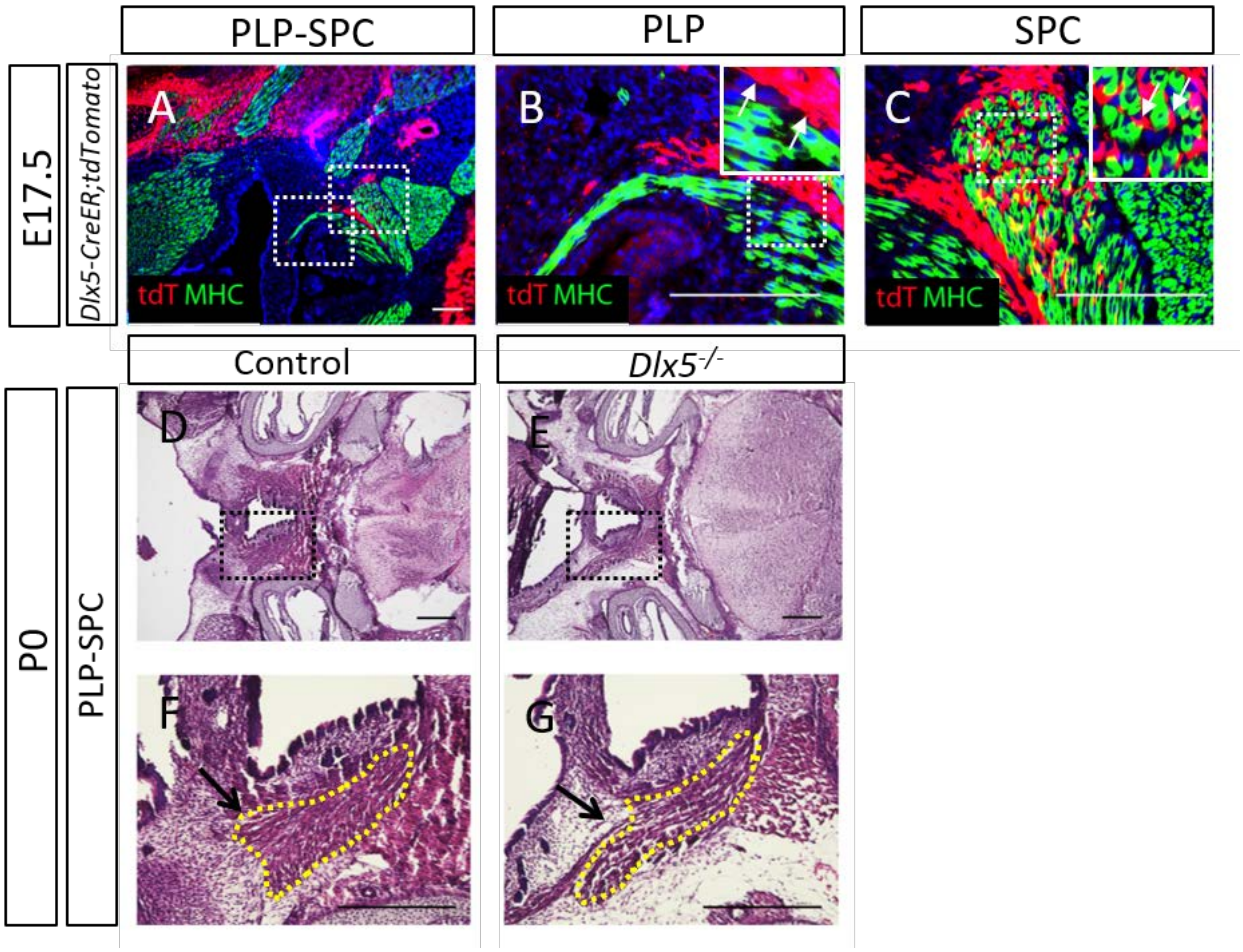

Fig. S1. Loss of Dlx5 affects the development of the superior pharyngeal constrictor muscle. (A-C) Visualization of tdTomato (tdT, red) and immunostaining of myosin heavy chain (MHC, green) in transverse sections of *Dlx5-CreER;tdTomato* embryos at E17.5. B and C are magnified images from white dotted boxes in A. Inserts in B and C are magnified images from white dotted boxes. White arrows indicate Dlx5-positive cells immediately adjacent to myogenic cells.(D-G) Hematoxylin and eosin staining of transverse sections of the soft palate at the level of the SPC in newborn control and *Dlx5*$^{-/-}$ mice. F and G are magnified images from dotted boxes in D and E, respectively. Yellow dotted lines indicate the location of the SPC based on our previous report (Grimaldi et al., 2015). Arrows indicate the area of the SPC in control mice with defects in *Dlx5*$^{-/-}$ mice. PLP, palatopharyngeus; SPC,superior pharyngeal constrictor. n=3. Scale bars: 500 µm in A-C; 250 µm in D-G.

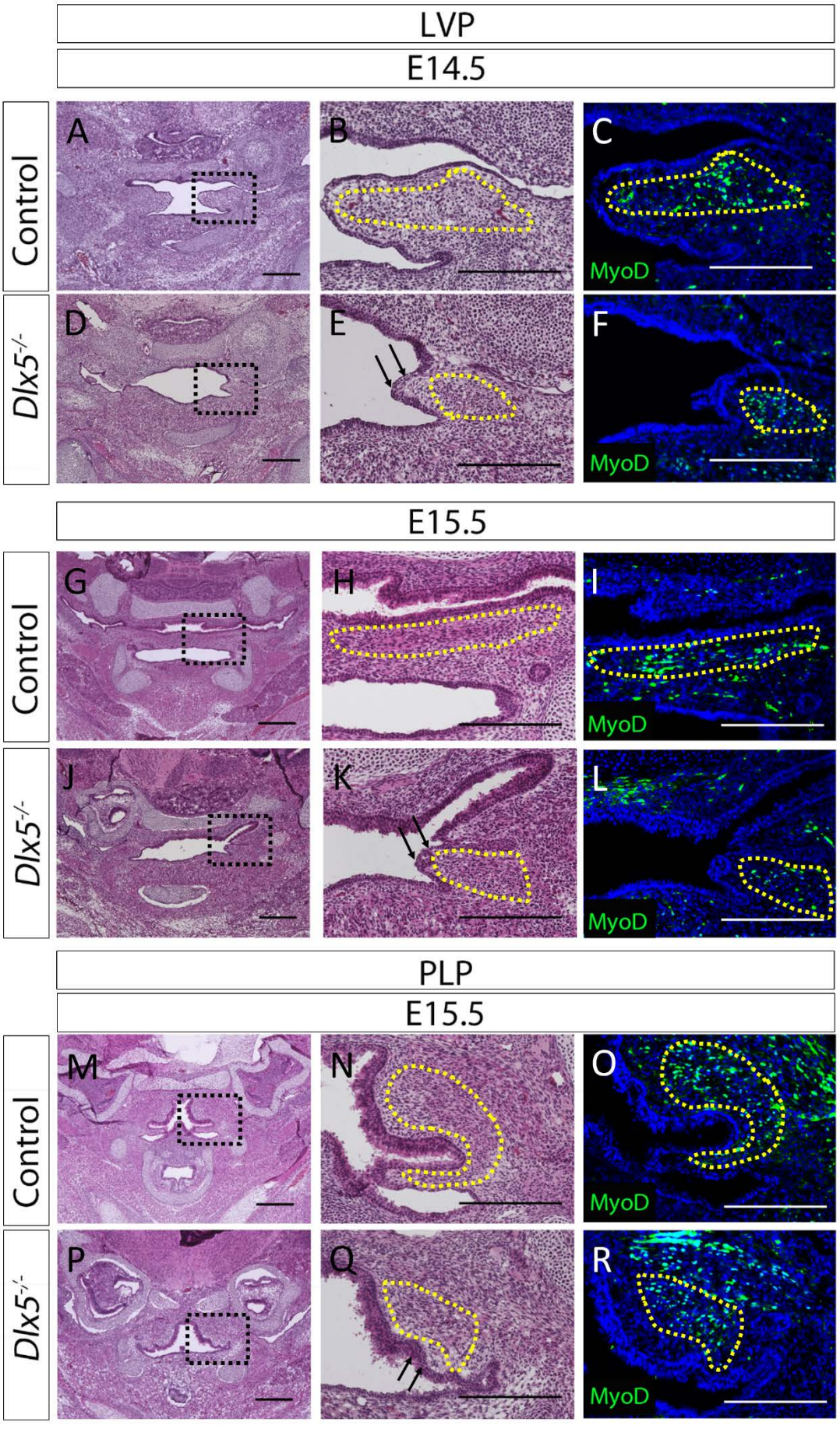

Fig. S2. Loss of Dlx5 leads to defects of the LVP and PLP. Hematoxylin and eosin staining and immunostaining of myoblast determination protein 1 (MyoD, green) in sections of the soft palate at the level of the LVP at E14.5 (A-F) and E15.5 (G-L), andthe PLP at E15.5 (M-R) in control and *Dlx5*$^{-/-}$ embryos.B/C, E/F, H/I, K/L, N/O and Q/R are magnified images from black dotted boxes in A, D, G, J, M and P, respectively. Yellow dotted lines indicate the LVP and PLP based on the area of MyoD-positive cells and our previous report (Grimaldi et al., 2015). Arrows indicate an absence of muscle tissue in *Dlx5*$^{-/-}$ mice. LVP, levator veli palatini; PLP, palatopharyngeus. n=3. Scale bars: 250 µm.

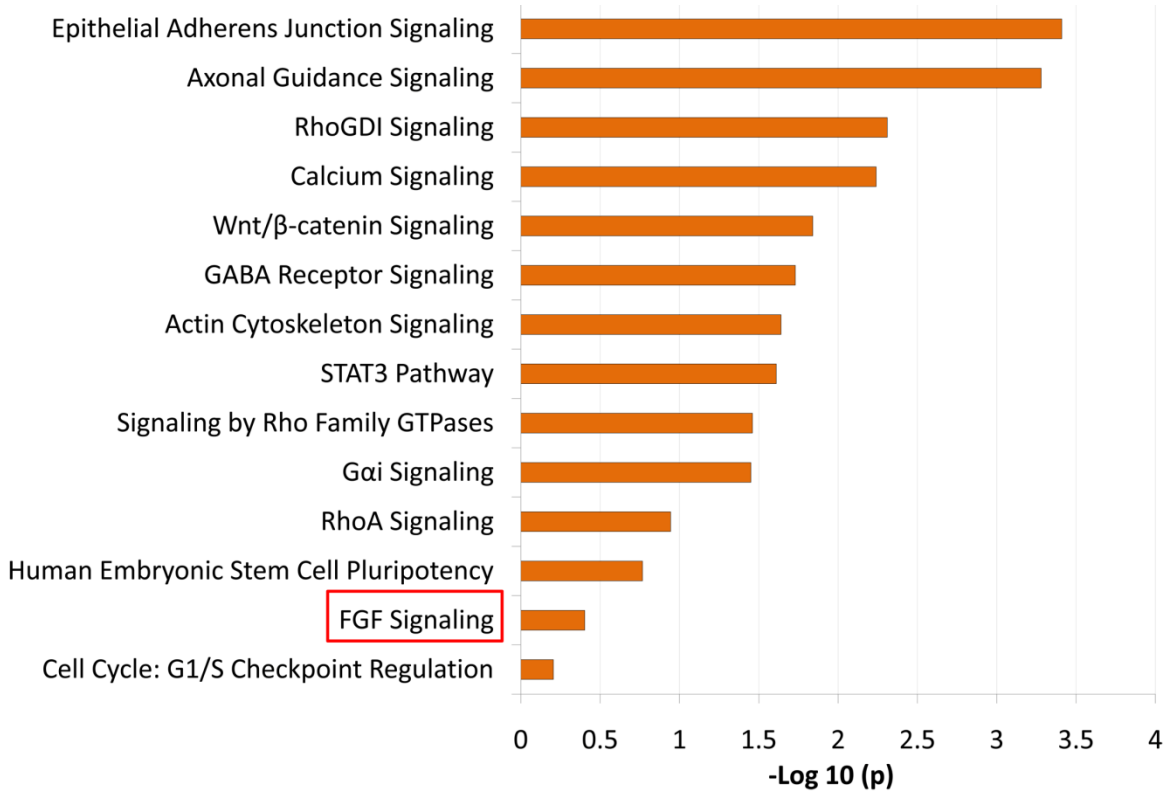

Fig. S3. Differential gene expression profile of soft palates of E14.5 *Dlx5*$^{-/-}$ mice. List of differentially expressed signaling pathways from RNA sequence analysis of the soft palate of E14.5 *Dlx5*$^{-/-}$ and control mice. Three samples per genotype were analyzed. n=3.

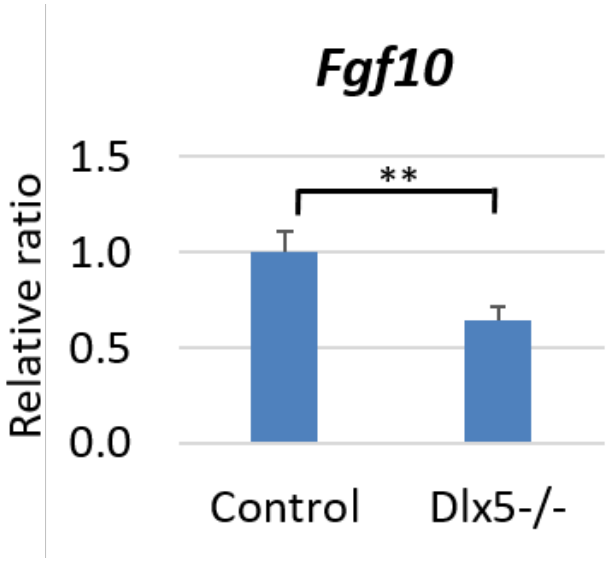

Fig. S4. Loss of Dlx5 leads to decreased gene expression of *Fgf10*. Quantitative RT-PCR analysis of *Fgf10* in the soft palate of E13.5 control and *Dlx5*$^{-/-}$ mice. Three samples per genotype were analyzed. **, $P<0.01$. n=3.

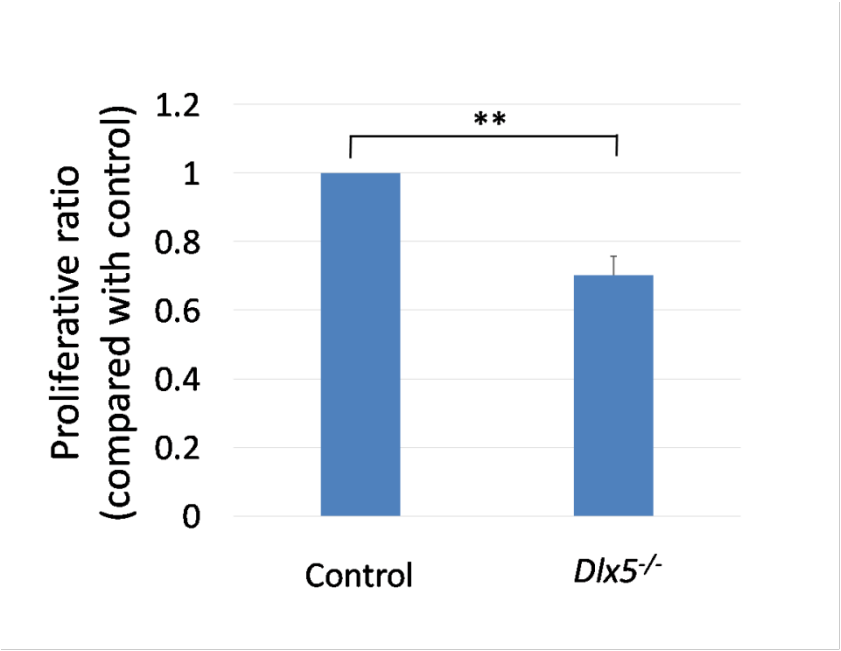

Fig. S5. Loss of Dlx5 leads to decreased proliferation in cells from soft palate muscles. Quantification of proliferation in cells from the soft palate of E13.5 control and *Dlx5*$^{-/-}$ embryos cultured with 2% horse serum for one week. Three samples per genotype were analyzed. **, $P<0.01$. n=3.